ELSEVIER

International Journal of Mass Spectrometry 220 (2002) 273–280

International Journal of Mass Spectrometry

www.elsevier.com/locate/ijms

Infrared spectra of the F^-–CH_4 and Br^-–CH_4 anion complexes

D.A. Wild, Z.M. Loh, E.J. Bieske*

School of Chemistry, University of Melbourne, Parkville, Vic. 3010, Australia

Received 20 November 2001; accepted 15 January 2002

Abstract

Infrared spectra are obtained for the F^-–CH_4 and Br^-–CH_4 anion complexes in the region of the C–H stretch vibrations of the CH_4 sub-unit. Spectra of both species exhibit two bands in the 2500–3000 cm^{-1} range. One band, a perpendicular transition distinguished by characteristic Q branches, is slightly red shifted from the $\nu_3(t_2)$ band of CH_4 ($\Delta\nu = -68\,cm^{-1}$ for F^-–CH_4 and $-34\,cm^{-1}$ for Br^-–CH_4). The other band, a parallel transition, corresponding mainly to vibrational motion of the hydrogen-bonded proton, is red shifted from the $\nu_1(a_1)$ transition of CH_4 ($\Delta\nu = -380\,cm^{-1}$ for F^-–CH_4, and $-31\,cm^{-1}$ for Br^-–CH_4). The spectra are compatible with C_{3v} structures for the F^-–CH_4 and Br^-–CH_4 dimers, whereby the halide anions are hydrogen-bonded to the CH_4 molecule through a single C–H unit. (Int J Mass Spectrom 220 (2002) 273–280)

Keywords: Infrared spectra; Charged complexes; Halide–methane complexes; Anion clusters; Negatively charged clusters

1. Introduction

Infrared spectra of charged complexes and clusters provide fundamental information on ion–neutral interactions. While spectroscopic studies initially focused on positively charged complexes, more recently anion complexes, particularly those whose cohesion is due to hydrogen bonds, have also been subject to spectroscopic attention. The studies show that the manner in which simple atomic and molecular anions are micro-solvated depends critically on the properties of the solvent molecules. For example, on the basis of infrared spectra and ab initio calculations, it has been established that the smaller Cl^-–$(H_2O)_n$, Br^-–$(H_2O)_n$, and I^-–$(H_2O)_n$ clusters have asymmetric structures in which the halide anion resides on the surface of a hydrogen-bonded water network [1–4]. The stability of such structures depends on the ability of each water molecule to act simultaneously as a proton donor to the halide anion and to another water molecule, as well as serving as a proton acceptor. The Cl^-–$(C_2H_2)_n$, Br^-–$(C_2H_2)_n$, and I^-–$(C_2H_2)_n$ complexes provide an interesting contrast to the hydrated halides, with infrared spectra suggesting that symmetric interior solvation structures are favoured [5–7]. In the smaller X^-–$(C_2H_2)_n$ clusters, roughly equivalent acetylene molecules are hydrogen-bonded end-on to the halide core in such a way that they are precluded from establishing bonds with one another. Progress has also been achieved in spectroscopically characterising cluster systems comprising halides hydrogen-bonded to other simple "solvent" molecules (including H_2 [8,9], CH_4 [10], NH_3 [11], and CH_3OH [12]).

To enhance our understanding of fundamental interactions between halide anions and small neutral molecules we have, in the current study, employed infrared

* Corresponding author. E-mail: evanjb@unimelb.edu.au

1387-3806/02/$ – see front matter
PII S1387-3806(02)00771-6

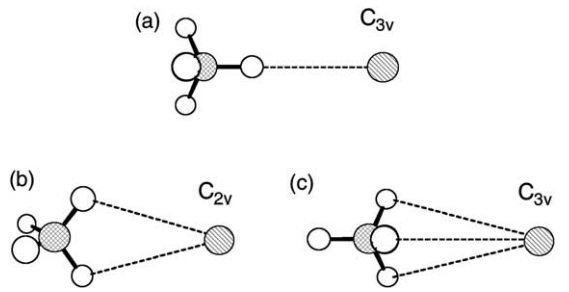

Fig. 1. Structures for the halide–methane complexes. The C_{3v} hydrogen-bonded structure (a) is predicted to lie lowest in energy, while the C_{2v} edge (b) and C_{3v} face (c) bound structures are predicted to be first and second order stationary points, respectively.

spectroscopy to investigate the F^-–CH_4 and Br^-–CH_4 dimers. Previous ab initio calculations [10,13] predict that the halide–methane complexes possess C_{3v} structures in which the halide is attached to the CH_4 sub-unit by a single hydrogen bond (Fig. 1(a)). Configurations in which the halide is attached by multiple hydrogen bonds to the edge or face of a distorted methane tetrahedron (Fig. 1(b) and (c)) are calculated to lie somewhat higher in energy. The theoretical binding energies are in reasonable accord with measured association enthalpies for F^-–CH_4 (27.9 kJ/mol), Cl^-–CH_4 (15.8 kJ/mol), Br^-–CH_4 (12.9 kJ/mol), and I^-–CH_4 (10.8 kJ/mol) [14]. Surprisingly even F^-, which normally establishes relatively strong bonds with H-bond donors, forms a comparatively weak link with CH_4. In contrast, the intermolecular bonds for the isoelectronic F^-–H_2O and F^-–NH_3 complexes are significantly stronger (with association enthalpies of 109.6 and 96 kJ/mol, respectively [15,16]).

The F^-–CH_4 and Br^-–CH_4 spectra, when considered together with the spectrum of Cl^-–CH_4 previously obtained by our group [10], allow us to systematically address questions relating to the structures of the halide–methane dimers. Do the complexes, as ab initio calculations suggest, possess the C_{3v} H-bonded structures shown in Fig. 1(a)? How well do existing ab initio calculations predict the spectra? What are the structural and spectroscopic consequences of changing the halide anion? How do the X^-–CH_4 spectra differ from those of complexes comprising halides bonded to other second row hydrides and how can these differences be related to other properties of the complexes?

2. Experimental methods

Due to the fragility of the halide–methane bonds, the X^-–CH_4 complexes are ideal candidates for interrogation in the C–H stretch region using infrared predissociation spectroscopy. As the measured binding energies [14] of F^-–CH_4 ($\approx$2350 cm^{-1}) and Br^-–CH_4 ($\approx$1085 cm^{-1}) lie below the vibrational energy of of the methane C–H stretch modes ($\nu_1(a_1)$ = 2914.2 cm^{-1} [17] and $\nu_3(t_2)$ = 3019.5 cm^{-1} [18]), delivery of vibrational energy into the methane sub-unit's C–H stretch modes should provide the dimers with sufficient energy to rupture the intermolecular bond, yielding detectable halide anion fragments.

The infrared spectra of mass selected F^-–CH_4 and $^{79}Br^-$–CH_4 complexes were recorded using a low energy tandem mass spectrometer apparatus [6]. The machine consists of a cluster ion source, a quadrupole mass filter for selection of the parent X^-–CH_4 complexes, a quadrupole bender that deflects the beam through 90° into a 60 cm long octopole ion guide, a second quadrupole mass filter for selection of the X^- photo-fragments, and an ion detector. While passing through the octopole guide, the ions encounter a counter-propagating IR beam, which, when tuned to an appropriate wavelength, serves to excite the complexes to predissociative (ro)vibrational levels resulting in the liberation of charged photo-fragments. Spectra were measured by monitoring the photo-fragment ion intensity as the infrared wavelength was scanned.

The F^-–CH_4 and Br^-–CH_4 complexes were synthesised in an electron beam crossed supersonic expansion. A 1:100 mixture of CH_4/Ar (8 bar) seeded with traces of either NF_3 (for F^-–CH_4) or CH_2Br_2 (for Br^-–CH_4) was expanded from a pulsed nozzle (0.8 mm orifice diameter, 40 Hz repetition rate) and crossed by 400 eV electrons issuing from twin rhenium filaments. The source design permits variation of the distance between the electron impact zone and

nozzle orifice to maximise cluster production. The F^- and Br^- anions are formed through dissociative attachment of electrons to NF_3 or CH_2Br_2, respectively. Subsequently, the halide ions are attached to CH_4 molecules through three-body association reactions in the early part of the supersonic expansion.

Tuneable infrared light was produced using a Nd:YAG laser pumped optical parametric oscillator (OPO) capable of generating light in the 2500–6900 cm^{-1} range with a bandwidth of $\approx$0.017 cm^{-1}. Wavelength calibration was accomplished using a wavemeter (New Focus 7711), through wavelength measurements of the visible output from the first stage of the OPO and 532 nm output of the seeded Nd:YAG pump laser. The pulsed ion source was run at twice the laser repetition rate so that laser on/off background subtraction could be used to account for collisional and metastable fragmentation.

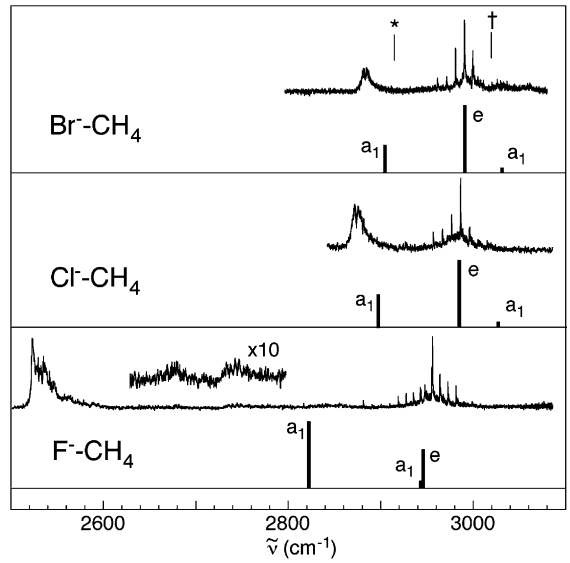

Fig. 2. Infrared spectra of the F^-–CH_4, Cl^-–CH_4, and Br^-–CH_4 complexes in the C–H stretch region. The calculated stick spectra are generated using the ab initio vibrational data from [13] with the frequencies scaled by 0.921. The $\nu_1(a_1)$ and $\nu_3(t_2)$ bands of the bare CH_4 molecule are denoted by an asterisk and a dagger, respectively. Note that the intramolecular vibrational states of the X^-–CH_4 complexes are labelled according to their CH_4 parentage and symmetry species in the C_{3v} point group.

3. Results

3.1. Vibrational structure of the spectra

The infrared spectra of the F^-–CH_4, Cl^-–CH_4, and Br^-–CH_4 dimers are displayed in Fig. 2. The spectrum of Cl^-–CH_4, which was reported in an earlier publication [10], is included for comparison. Each of the three spectra exhibits two prominent transitions. The higher frequency band is distinguished by sharp Q branches and has the form expected for a perpendicular transition of a prolate symmetric top. The frequency of this band, which is displaced to slightly lower energy from the $\nu_3(t_2)$ triply degenerate C–H stretch vibration of the free CH_4 molecule (3019.5 cm^{-1}), is relatively insensitive to the identity of the attached halide. The lower frequency band, which has the characteristic shape of a parallel transition (with a discernible band gap for Cl^-–CH_4, and Br^-–CH_4), is shifted to lower energy from the $\nu_1(a_1)$ symmetric C–H stretch band of CH_4 (2914.2 cm^{-1}). In contrast to the perpendicular band, the frequency of the parallel band depends strongly on the identity of the attached halide. Wavenumbers and assignments for prominent features in each of the three spectra are summarised in Table 1.

The frequencies and intensities of the vibrational bands in the F^-–CH_4, Cl^-–CH_4, and Br^-–CH_4 spectra are generally compatible with previous ab initio calculations [10,13], which forecast that the halide anions are attached to a single C–H group of the methane sub-unit through a linear hydrogen bond (Fig. 1(a)). Complexation with a halide anion reduces the symmetry of the tetrahedral methane molecule to C_{3v} whereupon the triply degenerate $\nu_3(t_2)$ C–H stretch vibrational mode is split into two infrared active C–H stretch modes, one of e symmetry (designated here as $\nu_3(e)$), and the other of a_1 symmetry (designated here as $\nu_3(a_1)$). These two vibrations mainly involve motion of the non-bonded hydrogen atoms. As well, the IR forbidden $\nu_1(a_1)$ symmetric stretch vibrational mode of CH_4 is rendered IR active to give an a_1 symmetry mode (designated here as $\nu_1(a_1)$) predominantly

Table 1
Wavenumbers (in cm^{-1}) for bands and Q branch peaks of F^-–CH_4 and Br^-–CH_4. The Q branch wavenumbers have ≈0.5 cm^{-1} uncertainties

Assignment		F^-–CH_4	Br^-–CH_4
$\nu_1(a_1)$	Head	2522.0 ± 0.5	
	Origin	2535	2883
$\nu_3(e)$	$^PQ_9$	2881.2	
	$^PQ_8$	2890.8	
	$^PQ_7$	2900.5	
	$^PQ_6$	2910.0	
	$^PQ_5$	2919.0	
	$^PQ_4$	2927.6	
	$^PQ_3$	2935.4	2961.4
	$^PQ_2$	2942.6	2971.2
	$^PQ_1$	2947.8	2980.9
	$^RQ_0$	2956.0	2990.6
	$^RQ_1$	2964.0	2999.5
	$^RQ_2$	2972.8	3007.9
	$^RQ_3$	2981.5	3016.8
	$^RQ_4$	2990.5	
	$^RQ_5$	2999.2	
	$^RQ_6$	3008.0	

Uncertainties in the $\nu_1(a_1)$ band positions are estimated to be ±5 cm^{-1}.

involving stretching motion of the hydrogen-bonded proton.

Stick spectra of the X^-–CH_4 complexes based on the ab initio calculations from [13], with frequencies scaled by the factor (0.921) required to bring the calculated CH stretch frequencies for bare CH_4 into line with the experimental values, are displayed in Fig. 2. The matches between the predicted and observed $\nu_3(e)$ perpendicular band positions for the three complexes are good, with the calculations nicely reproducing the observed halide-dependent red shift (e.g., $F^- > Cl^- > Br^-$). The $\nu_3(a_1)$ band, corresponding mainly to the symmetric stretching vibration of the three non-bonded protons, which is predicted to lie nearby the $\nu_3(e)$ perpendicular transition, is not apparent in any of the three spectra. However, the transition is predicted to be weak and may be concealed by the wing of the $\nu_3(e)$ band. It is worthwhile noting that ab initio calculations for Cl^-–CH_4 at the MP2(full)/aug–cc–VTZ level reported in [10] predicted similar intensities and frequencies for the $\nu_3(e)$ and $\nu_3(a_1)$ bands. However, the weak $\nu_1(a_1)$ band was predicted to lie somewhat lower in frequency than given by Novoa et al. [13].

There is a much less satisfactory agreement between experiment and theory for the $\nu_1(a_1)$ bands (corresponding to vibration of the hydrogen-bonded C–H stretch). For Cl^-–CH_4 and Br^-–CH_4 the $\nu_1(a_1)$ frequency is slightly overestimated by the calculations (by ≈20 cm^{-1} in each case) and massively overestimated for F^-–CH_4 (by ≈285 cm^{-1}). While we can offer no definite explanation for the large discrepancies, it seems most probable that the stretching potential for the hydrogen-bonded C–H group has a large degree of anharmonicity (particularly for F^-–CH_4). Similar, though more extreme, anharmonic effects have been observed in experimental and theoretical studies of the isoelectronic F^-–H_2O complex [19]. More reasonable theoretical estimates for the $\nu_1(a_1)$ frequencies may be obtainable using the vibrational self-consistent field (VSCF) method that has been successfully used to account for anharmonicities and intermode couplings in the isoelectronic Cl^-–H_2O complex [20,21].

The F^-–CH_4 spectrum contains two very weak bands (at ≈2680 and ≈2745 cm^{-1}) situated between the $\nu_1(a_1)$ and $\nu_3(e)$ transitions (see Fig. 2) for which only very tentative assignments can be offered. One possibility is that they are associated with overtones of the bending vibrational modes localised on the CH_4 sub-unit. In particular the overtone of the CH_4 $\nu_4(t_2)$ mode (which has a frequency of 1306 cm^{-1} [17]) occurs in the appropriate region. Alternatively, the bands may be due to combinations of $\nu_1(a_1)$ and the intermolecular stretching (ν_s) or bending (ν_b) modes. For example, assignment of the 2745 cm^{-1} band to the $\nu_1(a_1) + \nu_s$ combination would imply that ν_s has a frequency of ≈210 cm^{-1}, comparing favourably with the theoretical prediction of 199 cm^{-1} [13].

3.2. Structure of the $\nu_1(a_1)$ and $\nu_3(e)$ bands

Turning now to a discussion of structure of the individual vibrational bands, we note that the $\nu_1(a_1)$ bands of the F^-–CH_4, Cl^-–CH_4 and Br^-–CH_4 dimers are asymmetric, each displaying evidence for the formation of a P branch head. This is particularly evident

in the spectrum of F^-–CH_4. Existence of a P branch head implies that the *B* rotational constant increases upon vibrational excitation of the intermediate proton, and that the intermolecular bond contracts. The effect, which is a common feature of ionic hydrogen-bonded complexes, can be explained as arising from the vibrational dependence of the monomer electrical moments [22]. In the present case, vibrational excitation of the intermediate proton presumably enhances the vibrationally averaged local dipole moment of the hydrogen-bonded C–H group (due either to electrical or mechanical anharmonicity), leading to an increase in the electrostatic attraction with the halide anion.

The $\nu_3(e)$ perpendicular bands of F^-–CH_4, Cl^-–CH_4, and Br^-–CH_4 (plotted on an expanded scale in Fig. 3), contain a series of sharp peaks, corresponding to the ^RQ_K and ^PQ_K branches of a prolate symmetric top. If the most intense peak is assigned as the $^RQ_0$ transition, the Q branches follow the strong–weak–weak–strong intensity pattern expected for a prolate symmetric rotor containing three identical off-axis H atoms [17]. The $\nu_3(e)$ origins for F^-–CH_4, Cl^-–CH_4, and Br^-–CH_4 should lie approximately midway between the $^PQ_1$ and $^RQ_0$ peaks at around 2952, 2982, and 2986 cm^{-1}. The Q branch separations correspond reasonably well with theoretical predictions for the predicted minimum energy C_{3v} structures shown in Fig. 1(a). For a perpendicular transition of a prolate symmetric top the Q branch spacings are given by $2A'(1-\zeta_3)-2B'$, where ζ_3 is the Coriolis coupling coefficient for the ν_3 mode [17]. Assuming the calculated structural parameters from [13] and using the Coriolis coupling constant for the ν_3 mode of CH_4 ($\zeta_3 = 0.055$) [18], the Q branch spacings are calculated to be 9.7, 9.8, and 9.9 cm^{-1} for F^-–CH_4, Cl^-–CH_4, and Br^-–CH_4, comparing reasonably well with the observed spacings of approximately 8.2, 9.7, and 9.2 cm^{-1}.

Examination of the P and R branch regions of the $\nu_3(e)$ bands for each of the three complexes reveals evidence for resolved rotational substructure. As an example, Fig. 4 displays an expanded view of the region surrounding the strongest Q branch in the F^-–CH_4 spectrum ([10] contains a corresponding spectrum of Cl^-–CH_4). Individual rotational lines, with widths that are of the same order as the IR light bandwidth (≈0.017 cm^{-1}), are clearly apparent in the R branch. Unfortunately, assigning and analysing the

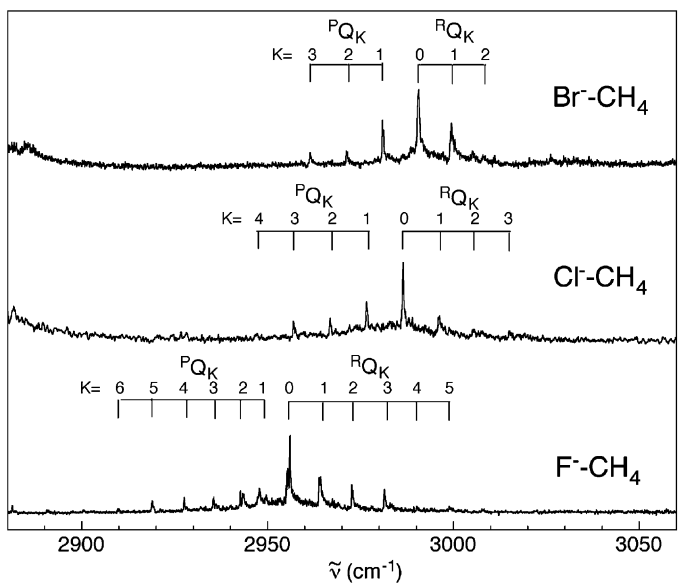

Fig. 3. Expanded view of the $\nu_3(e)$ perpendicular bands of F^-–CH_4, Cl^-–CH_4, and Br^-–CH_4. Wavenumbers for the Q branch peaks are summarised in Table 1.

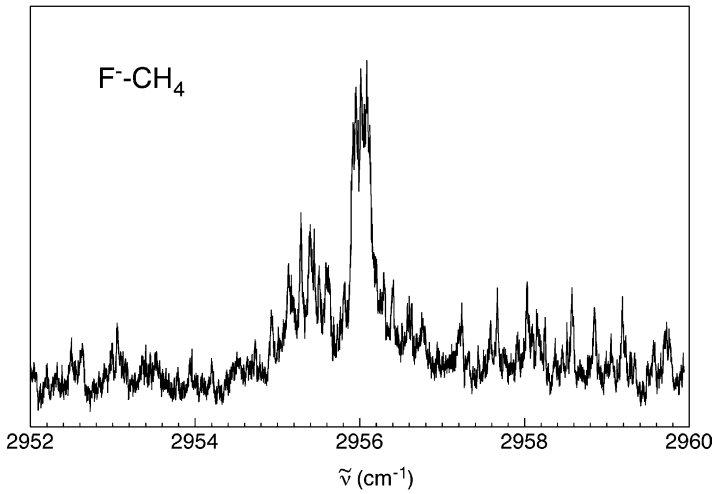

Fig. 4. Expanded view of the K = 1 ← K = 0 sub-band of F^-–CH_4. Clearly visible are R branch lines, with widths that are of the same order as the IR bandwidth (≈0.017 cm^{-1}).

P and R branch lines is thwarted by poor signal to noise ratio (particularly in the P branches).

4. Discussion

The X^-–CH_4 complexes, in which a halide anion is attached to a methane molecule through a single C–H hydrogen bond (Fig. 1(a)), can be viewed as stabilised intermediates for the proton transfer reactions

$$X^- + CH_4 \rightarrow XH + CH_3^-$$

As the proton affinities of F^-, Cl^-, and Br^- (1554.8, 1395, 1353.5 kJ/mol [23] and [24]) are considerably lower than that of CH_3^- (1743.5 kJ/mol [25]) the proton transfer reaction is endothermic. For this reason, the complexes are expected to be "reactant-like" such that the intermediate shared proton is primarily associated with the CH_3^- group, making it appropriate to regard them as a halide anion tethered to a perturbed methane molecule. Structures corresponding to the entrance channel complex of the highly endothermic S_N2 exchange reaction,

$$X^- + CH_4 \rightarrow CH_3X + H^-$$

in which the halide anion is located in the pocket between three C–H groups (Fig. 1(c)), are calculated to lie somewhat higher in energy, as are C_{2v} structures with double hydrogen bonds (Fig. 1(b)).

It is known through clustering equilibrium measurements and ab initio calculations that the halides establish much weaker ionic hydrogen bonds with CH_4 than with other second row hydrides. For example, the measured dissociation energies of F^-–CH_4, Cl^-–CH_4, and Br^-–CH_4 (2350, 1330, and 1085 cm^{-1}, respectively) [14] are substantially lower than the corresponding values for F^-–H_2O, Cl^-–H_2O, and Br^-–H_2O (9400, 5250, and 4550 cm^{-1}) [26,27]. The relatively low binding energies for the X^-–CH_4 complexes are reflected in the small red shifts in the frequencies of the hydrogen-bonded X–H stretch vibrations compared to the corresponding X^-–H_2O and X^-–NH_3 complexes. For example, the shifts of the bonded proton stretch bands for F^-–CH_4, Cl^-–CH_4, and Br^-–CH_4 are −380, −40, and −30 cm^{-1} (with respect to the $\nu_1(a_1)$ mode of bare CH_4 molecule), significantly less than the corresponding band shifts for F^-–H_2O, Cl^-–H_2O, and Br^-–H_2O (around −2000, −570, and −430 cm^{-1}, respectively) [19,28].

It is worth noting that the infrared spectra are compatible with the reported bond energies for the X^-–CH_4 complexes in the sense that the observed bands are relatively narrow, as would be expected if a single IR photon was sufficient to promote dissociation. In particular, the $\nu_1(a_1)$ band of F^-–CH_4 (anticipated to be the most strongly bound of the three complexes) is extremely intense and relatively narrow, evidence that cold complexes dissociate following deposition of $\approx$2550 cm^{-1} of vibrational energy. For this reason, it is probable that the band positions reported in Table 1 reflect the vibrational frequencies of cold complexes and are not unduly affected by the presence of vibrational hot bands. In future, this point can be explored by measuring spectra of X^-–CH_4 complexes to which one or more Ar "spy" atoms are attached, a strategy that has been profitably deployed to obtain infrared spectra of the more strongly bound hydrated halide anion complexes [28].

While there seems to be little doubt that the equilibrium configuration for the halide–methane dimers corresponds to the proton bound structure (Fig. 1), questions remain concerning the barriers for tunnelling between the four equivalent minima. The most facile tunnelling pathway is predicted to be through the bifurcated C_{2v} structure (Fig. 1(b)) [10,13]. The calculated barrier ($\approx$1070, $\approx$470, and $\approx$460 cm^{-1} for F^-–CH_4, Cl^-–CH_4, and Br^-–CH_4, respectively) is much larger than the rotational constant of the CH_4 sub-unit ($\approx$5.253 cm^{-1} [29]), so the internal rotation of the CH_4 sub-unit should be largely quenched. This is consistent with the fact that for each of the three complexes, the coarse Q branch structure of the $\nu_3(e)$ transition resembles that of a prolate symmetric top. Nevertheless, as demonstrated in studies of the Ar–NH_4^+ cation complex [30–32], the spectroscopic consequences of tunnelling are manifested in appreciable line splittings, even for relatively large barriers. In principle, rotationally resolved spectra in which the tunnelling splittings are resolved should provide information on the tunnelling barriers. However, as noted earlier, while the P and R branches in the $\nu_3(e)$ bands of all three dimers are partially rotationally resolved, at this stage analysis is precluded by the poor S/N ratio.

5. Conclusions

Infrared spectra of the F^-–CH_4 and Br^-–CH_4 dimers are reported. For both complexes, the spectra are consistent with structures in which the halide anion attached to the methane molecule through a single linear hydrogen bond, as predicted by earlier theoretical studies. Relatively small shifts in the frequencies of the C–H stretch vibrations with respect to those of the free CH_4 molecule, suggest that the X^-–CH_4 intermolecular bonds are comparatively weak, in agreement with previous thermochemical and theoretical studies. However, discrepancies between experimental and theoretical frequencies of the hydrogen-bonded C–H group (particularly for F^-–CH_4) suggest the need for further theoretical work. On the experimental front, rotationally resolved infrared spectra with improved signal to noise ratio should yield quantitative structural data for the X^-–CH_4 dimers, and provide information on the barriers separating equivalent minima on the intermolecular potential energy surface. It will also be interesting to record spectra of larger clusters to investigate the solvation of halide anions by methane molecules.

Acknowledgements

We are grateful to the Australian Research Council and the University of Melbourne for financial support.

References

[1] P.G.H. Ayotte, M.A. Johnson, J. Chem. Phys. 110 (1999) 7129.
[2] P. Ayotte, C.G. Bailey, G.H. Weddle, M.A. Johnson, J. Phys. Chem. 102 (1998) 3067.
[3] S.S. Xantheas, J. Phys. Chem. 100 (1996) 9703.
[4] J.-H. Choi, K.T. Kuwata, Y.-B. Cao, M. Okumura, J. Phys. Chem. 102 (1998) 503.
[5] P.S. Weiser, D.A. Wild, E.J. Bieske, Chem. Phys. Lett. 299 (1999) 303.
[6] P.S. Weiser, D.A. Wild, E.J. Bieske, J. Chem. Phys. 110 (1999) 9443.
[7] D.A. Wild, P.J. Milley, Z.M. Loh, P.S. Weiser, E.J. Bieske, Chem. Phys. Lett. 323 (2000) 49.

[8] D.A. Wild, P.S. Weiser, E.J. Bieske, A. Zehnacker, J. Chem. Phys. 115 (2001) 824.
[9] D.A. Wild, P.S. Weiser, E.J. Bieske, J. Chem. Phys. 115 (2001) 6394.
[10] D.A. Wild, Z. Loh, P.P. Wolynec, P.S. Weiser, E.J. Bieske, Chem. Phys. Lett. 332 (2000) 531.
[11] P.S. Weiser, D.A. Wild, P. Wolynec, E.J. Bieske, J. Phys. Chem. 104 (2000) 2562.
[12] O.M. Cabarcos, C.J. Weinheimer, T.J. Martinez, J.M. Lisy, J. Chem. Phys. 110 (1999) 9516.
[13] J.J. Novoa, M.-H. Whangbo, J.M. Williams, Chem. Phys. Lett. 180 (1991) 241.
[14] K. Hiraoka, T. Mizuno, T. Iiono, D. Eguchi, S. Yamabe, J. Phys. Chem. A 105 (2001) 4887.
[15] M. Arshadi, R. Yamdagni, P. Kebarle, J. Phys. Chem. 74 (1970) 1475.
[16] K.G. Spears, E.E. Ferguson, J. Chem. Phys. 59 (1973) 4174.
[17] G. Herzberg, Molecular Spectra and Molecular Structure, Vol. II, Infrared and Raman Spectra of Polyatomic Molecules, Krieger, Malabar, 1991.
[18] D.L. Gray, A.G. Robiette, A.S. Pine, J. Mol. Spectrosc. 77 (1979) 440.
[19] P. Ayotte, J.A. Kelley, S.B. Nielsen, M.A. Johnson, Chem. Phys. Lett. 316 (2000) 455.
[20] S. Irle, J.M. Bowman, J. Chem. Phys. 113 (2000) 8401.
[21] G.M. Chaban, J.O. Jung, R.B. Gerber, J. Chem. Phys. 111 (1999) 1823.
[22] E.J. Bieske, O. Dopfer, Chem. Rev. 100 (2000) 3963.
[23] C. Blondel, P. Cacciani, C. Delsart, R. Trainham, Phys. Rev. A 40 (1989) 3698.
[24] J.D.D. Martin, J.W. Hepburn, J. Chem. Phys. 109 (1998) 8139.
[25] G.B. Ellison, P.C. Engelking, W.C. Lineberger, J. Am. Chem. Soc. 100 (1978) 2556.
[26] P. Weis, P.R. Kemper, M.T. Bowers, S.S. Xantheas, J. Am. Chem. Soc. 121 (1999) 3531.
[27] M.M. Meot-Ner, S.G. Lias, in: P.J. Linstrom, W.G. Mallard (Eds.), Binding Energies between Ions and Molecules, and the Thermochemistry of Cluster Ions, NIST Chemistry WebBook, NIST Standard Reference Database Number 69, National Institute of Standards and Technology, Gaithersburg, MD, 20899 (http://webbook.nist.gov).
[28] P. Ayotte, G.H. Weddle, J. Kim, M.A. Johnson, J. Am. Chem. Soc. 120 (1998) 12361.
[29] G. Herzberg, Molecular Spectra and Molecular Structure, Vol. III, Electronic Spectra and Electronic Structure of Polyatomic Molecules, Krieger, Malabar, 1991.
[30] E.J. Bieske, S.A. Nizkorodov, O. Dopfer, J.P. Maier, R.J. Stickland, B.J. Cotterell, B.J. Howard, Chem. Phys. Lett. 250 (1996) 266.
[31] N.M. Lakin, O. Dopfer, M. Meuwly, B.J. Howard, J.P. Maier, Mol. Phys. 98 (2000) 63.
[32] N.M. Lakin, O. Dopfer, B.J. Howard, J.P. Maier, Mol. Phys. 98 (2000) 81.